



Published in final edited form as:

*J Phys Chem B*. 2012 January 12; 116(1): 690–697. doi:10.1021/jp210544w.

## The Case of Ketosteroid Isomerase

Stephen D. Fried<sup>1</sup> and Steven G. Boxer<sup>1</sup>

<sup>1</sup>Department of Chemistry, Stanford University, Stanford, CA 94305-5080

### Abstract

Structures of enzymes invariably reveal the proximity of acidic and basic residues to reactive sites on the substrate, so it is natural and common to suggest that enzymes employ concerted mechanisms to catalyze their difficult reactions. Ketosteroid Isomerase (KSI) has served as a paradigm of enzymatic proton transfer chemistry, and its catalytic effect has previously been attributed to concerted proton transfer. We employ a specific inhibitor that contains an IR probe that reports directly and quantitatively on the ionization state of the ligand when bound in the active site of KSI. Measurement of the fractional ionization provides a missing link in a thermodynamic cycle that can discriminate the free energy advantage of a concerted versus non-concerted mechanism. It is found that the maximum thermodynamic advantage that KSI could capture from a concerted mechanism ( $\Delta\Delta G^\circ = 0.5 \text{ kcal mol}^{-1}$ ) is quite small.

### Keywords

Enzyme catalysis; concerted acid-base catalysis; thermodynamic analysis; IR spectroscopy

## INTRODUCTION

Ever since the first crystallographic study of lysozyme<sup>1</sup>, the structure of an enzyme has been perceived as a window into the enzyme's mechanism. In particular, enzymes exhibit close contacts between reactive sites on the substrate and reacting residues of the enzyme in the Michaelis complex. These images often lead to the notion that enzyme-catalyzed reactions are highly concerted, involving multiple simultaneous bond-forming and bond-breaking events,<sup>2–10</sup> among other proposals. Concerted pathways are thought to avoid the formation of high-energy intermediates, thereby conferring great catalytic power.<sup>11,12</sup> Indeed, concerted mechanisms involving protons have been invoked in the mechanisms of many classic enzymes, such as the serine proteases,<sup>8</sup> ribonuclease,<sup>10</sup> and recently in the ribosome's peptidyl-transferase center.<sup>3</sup> However, there are other proposals that concerted mechanisms (i) are rare because they are generally not favorable except in limiting cases,<sup>13</sup> and (ii) are only used as a last resort when the transition state for the stepwise reaction is extremely unstable.<sup>12</sup> While kinetics may suggest the presence of a concerted or stepwise pathway, it is difficult to determine experimentally the energetic consequence of a concerted mechanism over its non-concerted analog, because in most instances only one of the two occurs. One may assume that the mechanism that *does* occur (whether it be concerted or not) is the most favored, but a more rigorous experimental comparison would be advantageous.

To whom correspondence should be addressed: Steven G. Boxer, Department of Chemistry, Stanford University, 380 Roth Way, Stanford, CA 94305-5080. Tel.: (650) 723-4482; Fax.: (650) 723-4817; sboxer@stanford.edu.

### ASSOCIATED CONTENT

Supplementary methods, synthesis, and results (including <sup>13</sup>C NMR studies) are included in the Supplementary Information. This material is available free of charge via the Internet at <http://pubs.acs.org>.

Ketosteroid Isomerase (KSI<sup>14</sup>) has served as a paradigm for enzymatic proton-transfer chemistry,<sup>15</sup> and is an ideal testing ground for evaluating the concerted catalysis idea because the proposal assumes the form of a simple question: what is the putative additional stabilization of a neutral dienol intermediate over a charged dienolate intermediate (Figure 1A)? We will demonstrate – consistent with some previous predictions<sup>16,17</sup> – that for KSI's reaction, a concerted mechanism would furnish only a very small thermodynamic advantage.

The KSI active site features an oxyanion hole (OAH) that poises two acidic moieties – Tyr16 and Asp103 – in close proximity to the oxygen atom of the substrate ketone.<sup>18,19</sup> The question is whether the OAH's function is to serve as a general acid (donating a proton to the intermediate) or as an electrophile (donating hydrogen bonds and stabilizing a charged intermediate). KSI's capacity to abstract a weakly-acidic  $\alpha$ -proton from its steroid substrate ( $pK_a = 12.7$ <sup>20</sup>) with its very weak general base ( $pK_a = 3.75$ <sup>21</sup>) has previously been attributed to concerted proton transfer, path (ii) in Figure 1B.<sup>18,22–25</sup>

The concerted pathway through Tyr16 is supported through four lines of evidence: structural, mutational, kinetic isotope effects, and theoretical. (i) A model of the substrate docked into the active site showed that Asp40 and Tyr16 approach the substrate most favorably in an approximately orthogonal geometry,<sup>18</sup> which is stereoelectronically optimal for a concerted enolization.<sup>26</sup> (ii) The decrease in  $k_{cat}$  suffered by KSI when both general base and putative general acid are ablated (Asp40Asn, Tyr16Phe;  $10^{9.8}$ -fold) is approximately additive with respect to the loss in activity upon removal of only the general base (Asp40Asn;  $10^{5.7}$ -fold) or only the putative general acid (Tyr16Phe;  $10^{4.7}$ -fold).<sup>18,22</sup> Additivity of rate effects is suggestive that the two residues act in concert. Because of its extreme effect on KSI's rate, its positioning, and its putative “matched”  $pK_a$ , Tyr16 is generally viewed as a better candidate for the general acid than the nearby Asp103. (iii) KSI exhibits a sizable primary kinetic isotope effect ( $6.13 \pm .30$ ) and a modest solvent isotope effect ( $1.59 \pm .10$ ), suggesting that chemistry involving the C4  $\beta$ -hydron and the Tyr16 hydroxyl hydron (which exchanges with solvent) are both rate limiting.<sup>23</sup> Moreover, the primary kinetic isotope effect at the 4 $\beta$  position is the same in D<sub>2</sub>O as in H<sub>2</sub>O, and the solvent isotope effect is the same for both the 4 $\beta$ -H and 4 $\beta$ -D substrates. These results indicate that the isotope effects are operational on the same chemical step, implying the rate-limiting step is a concerted process.<sup>23</sup> Many of these isotope effects are similar to those found for the enolization of acetone by acetate in solution, which also is believed to react in a concerted acid-base fashion.<sup>27</sup> (iv) Finally, Gerlt and Gassman discussed KSI in a series of papers that propose enzymes must use concerted proton transfer to overcome the enormous  $pK_a$  mismatch between their substrate acids and general bases.<sup>24,25</sup>

This position has been challenged by evidence from studies by Pollack et al. that have suggested the identity of the intermediate is a dienolate.<sup>28,29</sup> Fluorescence spectroscopy indicates that a non-reacting intermediate analog, equilenin, binds as its anionic form to the KSI active site,<sup>28</sup> and Brønsted analysis on a series of ligands produced a high  $\alpha$  ( $0.85 \pm 0.08$ ), consistent with charge residing largely on the ligand (rather than on Tyr16 or other OAH residues) in the complex.<sup>29</sup> Later experiments have cast some uncertainty on these claims: absorption studies of equilenin bound to a different homolog of KSI (from *Pseudomonas putida*) suggest it is present as a roughly 50/50 mixture of anionic and neutral forms,<sup>30</sup> and there is substantial disagreement between the measurements in ref. 29 and a more recent work that developed a more accurate binding assay.<sup>31</sup> In summary, there is experimental evidence for KSI's reaction intermediate being both a dienol and a dienolate<sup>18,22–30</sup> (Figure 1A), meaning the role of the OAH as a general acid or an electrophile has not been uniquely identified.

## Thermodynamic Model

To frame discussion, we will refer to a thermodynamic cycle (Figure 1B). The reaction labeled (i) is the aspartate-mediated proton abstraction. Reaction (ii) illustrates a concerted proton transfer pathway, in which an active site tyrosine is simultaneously deprotonated, resulting in the direct formation of a dienol intermediate. These processes can be compared by drawing in reaction (iii), which closes a thermodynamic cycle. Reaction (iii) corresponds to an internal proton transfer across the enzyme-substrate hydrogen bond; its reactant and product are the tautomers, E-O<sup>-</sup>•HO-L and E-OH•O-L, illustrated in red and blue in Figure 1C. The claim of the concerted acid-base hypothesis can be restated in terms of Figure 1B as  $\Delta G^\circ_{(ii)} < \Delta G^\circ_{(i)}$ . Thermodynamics requires that

$$\Delta G^\circ_{(iii)} = \Delta G^\circ_{(i)} - \Delta G^\circ_{(ii)}, \quad (1)$$

meaning that the internal proton transfer is a direct measure of the free energy advantage (the  $\Delta\Delta G^\circ$ ) of a concerted acid-base mechanism, (ii), over a simple base-mediated mechanism, (i).

## Approach

In practice, it is difficult to study reaction (iii) because treatment of the active enzyme with the true substrate results in an intermediate that persists for times on the order of a millisecond before quantitative conversion to the product state (E•P of Figure 1A). However, we can effectively isolate reaction (iii) from the other processes by treating the Asp40Asn mutant of KSI (KSI<sup>D40N</sup>), which simulates the protonated aspartic acid present in the E•I state, with an intermediate analog (Figure 1C). Note that both reaction (iii) and Figure 1C maintain a “neutral” general base through the reaction. Aromatic alcohols are frequently employed as intermediate analogs,<sup>29–31</sup> because they have  $pK_a$ s comparable to the true steroid dienol (10.0<sup>32</sup>) but have no way to tautomerize, so they effectively freeze the system in an E•I-like state. Specifically, phenols have been shown to bind to the KSI<sup>D40N</sup> active site and engage hydrogen bonds from OAH residues analogously to the A-ring of the true steroid substrate (31). By mimicking the hydrogen bond pattern the enzyme would use to stabilize the intermediate, these truncated ligands are able to achieve fairly high affinity to KSI<sup>D40N</sup> (2 – 100  $\mu$ M<sup>29,31</sup>). Moreover, remote binding interactions do not strongly affect KSI’s ability to perform the chemical steps of its mechanism,<sup>33</sup> suggesting mechanistic insights obtained for the truncated ligands likely apply to the full steroid. In order for the system illustrated in Figure 1C to properly simulate reaction (iii) of Figure 1B, the phenol needs to have precisely the same  $pK_a$  as the steroid dienol to accurately simulate its proton affinity<sup>30</sup>; this is possible with 4-fluorophenol (whose  $pK_a$  is also 10.0<sup>31</sup>), which also contains an intrinsic IR probe of protonation state. The  $\Delta G^\circ_{\sim(iii)}$  of Figure 1C can be determined by measuring  $f$ , the fraction of bound ligand ionized at equilibrium. Then, from the analogy drawn between (iii) of Figure 1B and  $\sim(iii)$  of Figure 1C, we assert  $\Delta G^\circ_{(iii)} = \Delta G^\circ_{\sim(iii)}$ , which completes the thermodynamic cycle in Figure 1B.

In earlier work,<sup>30</sup> the proton affinity of the active site of KSI was estimated by binding a series of naphthols whose solution  $pK_a$  varied from 8.4 to 10.1. The electronic spectrum of the neutral and ionized states of these naphthols was sufficiently different that their degree of ionization when bound at the active site could be estimated, though band overlap between these forms and non-trivial spectral shifts from the solution basis spectra precluded identification of two discrete states needed for the thermodynamic analysis, and compromised the accuracy of quantitation. We executed <sup>13</sup>C NMR studies (Figure S1) of phenolic ligands with a <sup>13</sup>C label at the carbon adjacent to the hydroxyl group to detect its

ionization state in the KSI active site. However, as described in detail in the Supplemental Information, ligand exchange dynamics and the convolution of effects from ionization and environment on the chemical shift compromise quantitative determination of  $\mathbf{f}$ . As shown in the following, IR probes can provide the needed combination of spectral separation and timescale to directly probe the ionization state of the ligand in the active site of KSI. These data provide a reliable estimate of  $\mathbf{f}$ , which can then be used to rigorously evaluate the thermodynamics of the internal proton transfer.

## EXPERIMENTAL PROCEDURES

### FTIR Spectroscopy

All spectra were recorded on a Bruker Vertex 70 FTIR spectrometer outfitted with a global blackbody source, a KBr beamsplitter, and a sample chamber connected to nitrogen tank to purge atmospheric gases. In general, the solution-state samples were loaded into a demountable liquid cell (Bruker) with two windows (CaF<sub>2</sub>, .750" thick, Red Optronics for C-F stretch; sapphire, .750" thick, Meller Optics for C-N stretch). The windows were separated using two off-set semicircular mylar spacers (12  $\mu\text{m}$  and 23  $\mu\text{m}$  for C-F stretch; 75  $\mu\text{m}$  and 100  $\mu\text{m}$  for C-N stretch). The rather short pathlength was needed for the C-F region due to high extinction from water). In order to maximize signal, a band-pass interference filter (Spectrogon) was used in order to block light outside the region of interest (1000–1500  $\text{cm}^{-1}$  germanium band-pass for C-F; 2000–2500  $\text{cm}^{-1}$  sapphire band-pass for C-N). For the C-F stretch, a typical liquid N<sub>2</sub> cooled MCT detector was employed; however, for the C-N stretch, a liquid N<sub>2</sub> cooled InSb detector was more appropriate. For each run, 256 scans were acquired over a 500  $\text{cm}^{-1}$  range at 1  $\text{cm}^{-1}$  resolution, and then averaged to furnish each transmission interferogram. The interferograms were subject to apodization by a Blackman-Harris function, phase correction by a power spectrum method, and fast Fourier transformation to generate the spectrum. An identical procedure was employed to acquire a transmission spectrum of the appropriate background sample (see details below). Absorption spectra were calculated from the log-difference of the sample and background transmissions, and were subsequently cut and baselined using a polynomial fit. Band positions and FWHMs were calculated using the OPUS software (Bruker), which uses a second-derivative-based method. When lineshapes were fit, a Levenberg-Maquardt algorithm was used from the OPUS software. Each experiment was repeated in triplicate. The three repeats from the separate runs were averaged together to furnish the spectra that are given in figures.

**FTIR Backgrounds**—In order to obtain high-quality spectra in the C-N region, a fairly simple background suffices because proteins have no intrinsic absorption near 2000  $\text{cm}^{-1}$ . An aliquot of crystalline lysozyme (Sigma-Aldrich) was dissolved in an aqueous buffer, 40 mM KPi, pH 7.2. The concentration of lysozyme was made to approximately match that of KSI from the sample in units of mg/mL. On the other hand, obtaining clean spectra in the C-F region is considerably more difficult, as proteins possess complex vibrational structure in this region, and so a ligand-editing procedure was employed. A typical sample was prepared by mixing 15  $\mu\text{L}$  of KSI<sup>D40N</sup> (4.7 mM, 40 mM KPi, pH 7.2) with .46  $\mu\text{L}$  of fluorophenol ligand (100 mM, DMSO). The corresponding background would be prepared by mixing 15  $\mu\text{L}$  of KSI<sup>D40N</sup> from the same stock to .46  $\mu\text{L}$  of phenol (100 mM, DMSO). This nearly identical background cancels out all the signal in the absorption spectrum except due to the C-F band. To obtain high-quality spectra, we also found that: (1) sample and background spectra had to be acquired on the same day, preferably back-to-back, and (2) care needed to be taken to screw down the screwcap of the liquid demountable cell with the same number of turns to make the pathlengths match as closely as possible.

Preparation and isolation of KSI, synthesis of non-commercially available ligands, and  $^{13}\text{C}$  NMR methods are described in the supplementary methods of the Supplementary Information.

## RESULTS

In order to simulate process (iii) in Figure 1B we sought an IR probe on a phenolic ligand whose  $\text{p}K_a$  is as close as possible to the steroid dienol, and where the neutral and ionized basis spectra are well-defined and well-separated. Previous work has employed the C-D stretch to assess ionization states in proteins<sup>34,35</sup>; unfortunately we found that the C-D bands of deuterated phenols were too broad (FWHM  $20\text{ cm}^{-1}$ ) and weak ( $\epsilon \cdot 10\text{ M}^{-1}\text{ cm}^{-1}$ ) to be suitable for our application.

The C-F stretch is an intense IR band typically at  $1200\text{ cm}^{-1}$  (36), which can be distinguished from the protein background with proper precaution using the technique of ligand editing. 4-fluorophenol was a promising candidate for the present study. It has a  $\text{p}K_a$  of 10.0<sup>31</sup> and a  $22\text{ cm}^{-1}$  shift accompanying ionization (Figure 2B, Table 1). However, neutral 4-fluorophenol's spectrum in the C-F stretch region (Figure 2B) is complicated by the presence of an overtone at  $1200.6\text{ cm}^{-1}$ , in Fermi resonance with the C-F band.<sup>37</sup> As shown in Figure 2A, the resonance is fairly weak in  $\text{CCl}_4$ , but grows considerably stronger in aqueous solution. The Fermi resonance complicates assigning one peak to one protonation state of the phenol because intensity at  $1200\text{ cm}^{-1}$  results from a superposition of the C-F band in the ionized state and the overtone resonance in the neutral state. The spectrum of 4-fluorophenol when bound to  $\text{KSI}^{\text{D40N}}$  (Figure 2C) shows two peaks at  $1221.9\text{ cm}^{-1}$  and  $1201.0\text{ cm}^{-1}$  of similar intensity, which cannot be reconstructed by any superposition of the aqueous basis spectra, suggesting the enzyme active site environment is also modulating the Fermi resonance. These complications led us to selectively deuterate 4-fluorophenol, expecting that it would remove the Fermi resonance.

Indeed, 4-fluorophenol-2,6- $d_2$  (4Fd2, Table 2) meets all the criteria delineated for this study. It possesses a simple spectrum in the region surrounding the C-F stretch (Figure 2D), and also has a fairly large ionization-induced shift ( $14.3\text{ cm}^{-1}$ , Figure 2E). IR spectra taken of the complex  $\text{KSI}^{\text{D40N}} \cdot 4\text{Fd2}$  (Figure 2F) show two bands positioned at  $1188\text{ cm}^{-1}$  and  $1171\text{ cm}^{-1}$ . We assign these to the neutral and ionized populations of 4Fd2, each slightly red-shifted from their solution values (Figure 2E), reflecting the influence of the KSI active site environment. The observation that appreciable populations of both tautomers exist in thermal equilibrium shows unambiguously that the neutral form is not greatly stabilized over an anionic form. The case for the two peaks in Figure 3F corresponding to two binding modes of the ligand can be ruled out because: (i) the crystal structures of phenol<sup>31</sup> (which has nearly the same  $\text{p}K_a$  and steric features as 4Fd2) as well as of 3-fluoro-4-nitrophenol bound to  $\text{KSI}^{\text{D40N}}$  both furnish density of only a single binding mode (unpublished results), and (ii) as shown in Figure 3, when a parallel study is conducted on the C-N stretch of  $\text{KSI}^{\text{D40N}}$ -bound 4-cyanophenol ( $\text{p}K_a = 7.95$ ,  $K_D = 6\text{ }\mu\text{M}^{29}$ ), only the expected<sup>30</sup> deprotonated state is observed in the spectrum (Table 1). This provides a key control for the method (two peaks only appear if two ionization states are appreciably populated), but has no direct relevance to Figure 1B because 4-cyanophenol is much more acidic than the steroid dienol. Furthermore, as shown in Figure 4 (details given in Table S3), changing concentrations of  $\text{KSI}^{\text{D40N}}$  or 4Fd2 produced borrowing or adding intensity to the (de)protonated populations as anticipated. These results strongly indicate the simultaneous presence of the two tautomers,  $\text{E-O}^- \cdot \text{HO-L}$  and  $\text{E-OH} \cdot \text{O}^- \text{-L}$ , in equilibrium. The task to determine **f** from the IR spectra involves a quantitative assessment of the population associated with each peak.

Relative populations ( $p_n$ ) are found by referencing each peak's integrated intensity to the oscillator strength of the corresponding basis state, namely:

$$p_n = \frac{I_n^{KSI}}{I_n^{ref}} \quad (2)$$

where  $n$  indexes ionization state of 4F*d*2 (1 = neutral; 2 = anionic),  $I_n^{KSI}$  is the integrated intensity of a C-F peak in the protein (Figure 2F), and  $I_n^{ref}$  is the integrated intensity of the basis spectrum of neutral or ionized 4F*d*2 (Figure 2E). We note that equation (2) assumes that the intensity of a transition is unperturbed by the active site environment. This assumption appears valid, as the sum of the two referenced intensities in the KSI<sup>D40N</sup>-bound spectrum (Figure 2F, Table 2) is 1.04, quite close to unity. The doubly-peaked spectra of KSI<sup>D40N</sup>•4F*d*2 (Figure 4) were fit to two Gaussians using the OPUS software package with the Levenberg-Marquardt algorithm (Figure 2F, red and blue traces). The Gaussian fits were integrated to give the integrated intensities,  $I_n^{KSI}$ . The integrated intensities were referenced (according to equation (2)) to give relative populations of the ionization states,  $p_n$  (1 = neutral; 2 = anionic). A simple ratio of the populations

$$f_{obs} = p_2 / (p_1 + p_2) \quad (3)$$

can be used to determine  $f_{obs}$  (the overall fraction ionized). However, at any concentration, some ligand will remain free in solution, where it will be protonated ( $pK_a^{4F*d*2} \gg pH$ ). The fraction of 4F*d*2 that is bound to KSI,  $f_{bound}$ , can be determined from the binding constant ( $K_D = 150 \mu M^{31}$ ); therefore we can remove the contribution of the non-bound ligand to obtain  $f$ :

$$f = \frac{p_2}{\frac{I_1^{KSI} - (1 - f_{bound})I_1^{ref}}{I_1^{ref}} + p_2} \quad (4)$$

Figure 4 shows that when KSI concentration is lowered (red trace), a greater portion of 4F*d*2 is displaced into solution, causing some intensity in the ionized population to shift into the neutral population. When the 4F*d*2 concentration is raised well over the KSI concentration (blue trace), the additional signal appears in the neutral population.  $f_{obs}$  decreases because of the presence of free (neutral) 4F*d*2, but it is important to note that equation (4) can accurately account for free 4F*d*2, causing the calculated value of  $f$  to be similar. We determine that the fraction ionized of ligand when bound,  $f$ , is  $0.30 \pm .02$  – consistent with our prior study using UV-Vis spectroscopy to estimate the proton affinity of the active site.<sup>30</sup> Our reported value of  $f$  as 0.30 is based on the fact that we feel most confident in the data where the most 4F*d*2 is bound (black trace of Figure 4), but we use the other two conditions along with equation (4) for the purpose of estimating the error in the value. The <sup>13</sup>C NMR approach – as described in the Supplementary Data – can be extrapolated to give a relatively consistent value, but not a direct measurement.

## DISCUSSION

While <sup>13</sup>C NMR methods are ideal for performing site-specific titrations in proteins,<sup>38–40</sup> we found it less adequate to provide an accurate measure of the fraction ionized because the observed chemical shift convolutes ionization with environment effects from the active site,



an ongoing problem in the analysis of chemical shifts.<sup>41</sup> These observations highlight the difficulty in identifying incisive probes of internal proton transfers for the general reason that many spectroscopic observables convolve environmental effects and ionization. IR methods offer an intrinsically fast timescale that affords observation of the two states of the internal proton transfer as two separate populations, and so circumvents the problem of ionization/environment convolution, and with a probe like 4F*d*2 avoids the uncertainty of strongly overlapping bands. For present purposes, we consider the value of **f** determined from IR spectroscopy to be the most reliable, and with this information in hand, we return to the thermodynamic analysis in Figure 1B.

According to chemical equilibrium,

$$\begin{aligned}\Delta G_{(iii)} &= \Delta G^\circ_{(iii)} + RT \ln \left( \frac{[\text{E} - \text{OH} \bullet \text{O}^- - \text{L}]}{[\text{E} - \text{O}^- \bullet \text{HO} - \text{L}]} \right) \\ &= \Delta G^\circ_{(iii)} + RT \ln \left[ \frac{\mathbf{f}}{1 - \mathbf{f}} \right].\end{aligned}\quad (5)$$

The equilibrium state (where **f** = .30) corresponds to the state for which the free energy the system can dissipate is zero (i.e.,  $\Delta G_{(iii)} = 0$ ). Using equation (5), we determine that  $\Delta G^\circ_{(iii)}$  is  $0.5 \pm .05 \text{ kcal mol}^{-1}$ . According to equation (1),  $\Delta G^\circ_{(iii)}$  is equal to the amount of free energy saved by concerted proton transfer. We conclude that the maximum thermodynamic advantage that KSI could theoretically capture from a concerted mechanism ( $\Delta \Delta G^\circ = 0.5 \text{ kcal mol}^{-1}$ ) is quite small, compared to the overall stabilization of the intermediate as estimated from kinetics ( $\Delta \Delta G^\circ = 11 \text{ kcal mol}^{-1}$ ).<sup>15,17</sup> While the results show the thermodynamics of both mechanisms in Figure 1B are similar, evidence from solution studies suggests that their barriers may still differ.<sup>42</sup> We emphasize that our current study illustrates that neither mechanism can be favored or excluded on the basis of thermodynamics.

This result provides direct experimental evidence in support of the hypothesis of Guthrie and Kluger,<sup>16</sup> who posited that concerted catalysis is not generally favored in enzymology due to the possibility of electrostatic stabilization of charged states. More specifically, our result validates a suggestion made by Pollack that the “exact position of the proton is unimportant,” as the E-OH•<sup>-</sup>O-L and E-O<sup>-</sup>•HO-L states are so similar in free energy.<sup>17</sup>

Xue and coworkers<sup>43</sup> addressed the question that we posed with a different strategy. The KSI<sup>D40N</sup> mutant is capable of slowly enolizing its substrate (Figure 1A: E•S → E•I;  $k = .052 \text{ s}^{-1}$ ) but is effectively unable to turnover to product, allowing the intermediate-bound state to persist for hours, from which one observes both dienol and dienolate forms of the steroid with UV-Vis.<sup>43</sup> Xue found from relative intensities of the two maxima that the fraction of bound intermediate ionized, **f**, is between 0.6–0.8. That result is consistent with our own, noting that Xue’s study was conducted on a different homolog of KSI (that from *Comamonas testosteroni*), which has a higher proton affinity than the KSI studied here by 0.7 pK units.<sup>30</sup> This consistency in fractional ionization between phenols and steroids also helps to validate our approach of using truncated ligands to model the fractional ionization of a steroid. We note however that the UV-Vis methods employed in ref. 43 as well as in ref. 30 suffer from the difficulty of overlapping spectral features between different species, making assignments of species ambiguous and quantitation difficult.

These results and model also present an opportunity to comment on the classic libido rule of concerted acid-base catalysis,<sup>12</sup> which was based on a three-state thermodynamic cycle very reminiscent to Figure 1B. The libido rule states that a concerted acid-base mechanism is likely to impart a thermodynamic advantage when the candidate site of concerted proton transfer (in this case, the steroid’s ketone O-atom) undergoes a large change in  $\text{p}K_a$  over the

course of the mechanism, and when the  $pK_a$  of the catalyst (in this case, the enzyme's OAH) is intermediate between the two. KSI passes the libido rule, because the protonated ketone (see **E•S** in Figure 1A) is highly acidic (an oxocarbenium has  $pK_a$  ca.  $-2$ <sup>18</sup>), and the protonated enol (**E•I**) is quite unacidic ( $pK_a$  10.0). The  $pK_a$  of the oxyanion hole of KSI<sup>D40N</sup> has recently been found ( $6.3 \pm 0.1$ <sup>44</sup>), and it is intermediate between the two  $pK_a$ s of the ligand's O-atom. Based on these  $pK_a$ s, the libido rule predicts KSI would benefit from a concerted acid-base mechanism, whereas our results and others'<sup>17,43</sup> suggest otherwise. This inconsistency suggests that the  $\Delta G^\circ$ s of processes (i)–(iii) in Figure 1B cannot be accurately expressed in terms of  $pK_a$ . This is perhaps not surprising, because  $pK_a$  corresponds to transfer of protons between a given species and *water*, and *none* of the reactions (i)–(iii) in Figure 1B involve proton transfers to water, so their free energies are not straight forward to ascertain from  $pK_a$ s alone. In Figure 1B, we avoided using  $pK_a$ s to construct energetic relationships between the various states, in preference of the more fundamental measure, **f**. Indeed the value of **f** we measured (0.30) is not consistent with the relative  $pK_a$  between oxyanion hole (6.3) and dienol (10.0) which would imply **f** to be  $\sim 0$ .

We note two broader consequences of this work. Firstly, the result suggests that the frequently encountered “stepwise vs. concerted” dichotomy may not always be the most relevant focus for dissecting the thermodynamic contributions to enzymatic proton-transfer catalysis, and at the very least, a concerted mechanism should not be equated with a large intermediate stabilization, as sometimes supposed.<sup>24,25</sup> Secondly, evidence that a reaction follows a concerted mechanism<sup>18,22–23</sup> does not imply the conclusion that concertedness is indispensable for the reaction to take place. We suggest that a concerted mechanism may not necessarily be the most thermodynamically favorable way to perform a proton abstraction in general.

Interestingly, this same question has arisen in the pursuit of artificial enzymes of the Kemp elimination, which like KSI also must abstract a weakly-acidic proton. Researchers who sought to design Kemp eliminase *de novo* found that constructs bearing putative general acids were just as proficient or weaker than constructs without.<sup>45</sup> Furthermore, attempts to design a concerted proton transfer mechanism into an active catalytic antibody by incorporating a general acid residue destroyed the catalyst.<sup>46</sup> These observations are consistent with an emerging view critical of the concerted acid-base mechanism. Finally, we note that the presence of two peaks in Figure 2F implies that IR would be ideal to quantify effects that can perturb ionization populations, such as temperature, mutations, or an externally applied electric field. Through studies of this nature, the barrier to proton transfer across a coupled hydrogen-bond network could be ascertained, leading to deeper insights into the underlying dynamics of enzyme function.

## CONCLUSION

IR spectroscopy lends a combination of spectral separation and timescale to differentiate two protonation states in equilibrium, and by using specific IR probes, a single internal proton transfer can be observed in an entire protein. The data demonstrate unambiguously that two protonation states of an intermediate analog coexist in the active site of KSI. This information, in the context of a thermodynamic cycle, implies that the maximum thermodynamic advantage that KSI could capture from a concerted mechanism is only  $\Delta\Delta G^\circ = 0.5 \text{ kcal mol}^{-1}$ . Our study suggests that enzymes may not need to employ concerted acid-base mechanisms in order to catalyze difficult proton-transfer reactions.

## Supplementary Material

Refer to Web version on PubMed Central for supplementary material.



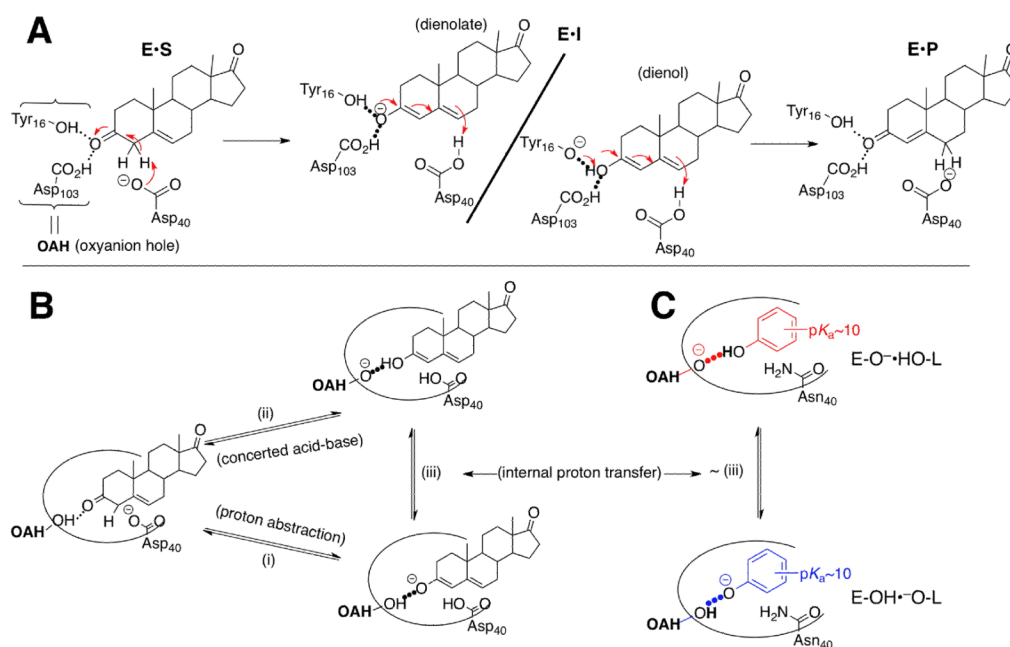
## Acknowledgments

SDF thanks the NSF for a pre-doctoral fellowship. This work is supported in part by a grant from the NIH (GM27738).

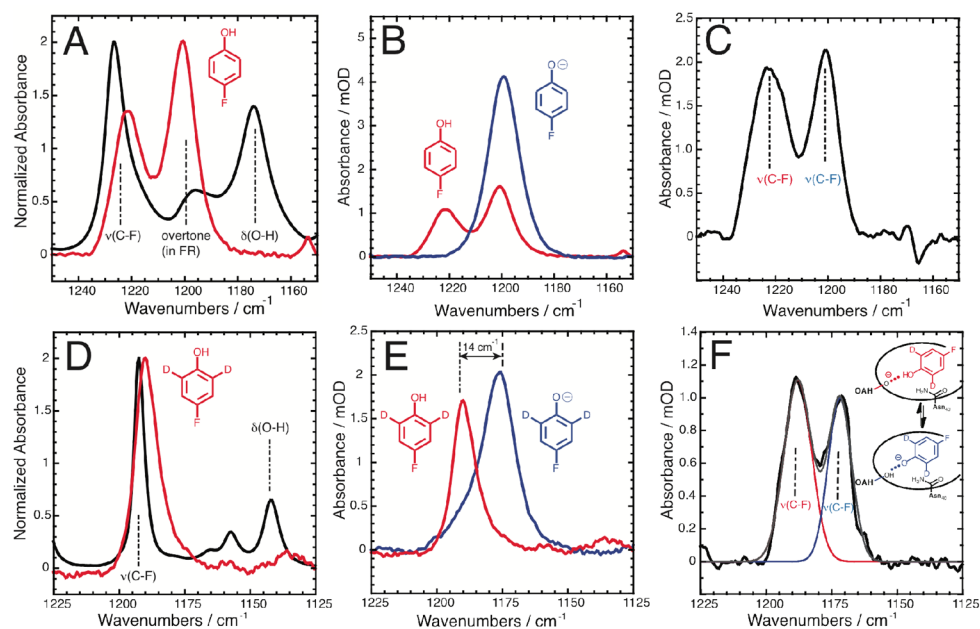
## References

1. Blake CCF, Johnson LN, Mair GA, North ACT, Phillips DC, Sarma VR. Proc Roy Soc London B. 1967; 167:378–388. [PubMed: 4382801]
2. Winkler A, Lyskowski A, Riedl S, Puhl M, Kutchan TM, Macheroux P, Gruber K. Nature Chem Biol. 2008; 4:739–741. [PubMed: 18953357]
3. Schmeing TM, Ramakrishnan V. Nature. 2009; 461:1234–1242. [PubMed: 19838167]
4. Fogle EJ, Toney MD. Biochim Biophys Acta. 2011; 1814:1113–1119. [PubMed: 21640851]
5. Tsybovsky Y, Donato H, Krupenko NI, Davies C, Krupenko SA. Biochemistry. 2007; 46:2917–2929. [PubMed: 17302434]
6. Sondek J, Lambright DG, Noel JP, Hamm HE, Sigler PB. Nature. 1994; 372:276–279. [PubMed: 7969474]
7. Engel CK, Mathieu M, Zeelen JP, Hiltunen JK, Wierenga RK. EMBO J. 1996; 15:5135–5145. [PubMed: 8895557]
8. Hunkapiller MW, Forgac MD, Richards JH. Biochemistry. 1976; 15:5581–5588. [PubMed: 999831]
9. Kirsch JF, Eichele G, Ford GC, Vicent MG, Jansonius JN, Gehring H, Christen P. J Mol Biol. 1984; 174:497–525. [PubMed: 6143829]
10. Findlay D, Herries DG, Mathias AP, Rabin BR, Ross CA. Biochem J. 1962; 85:152–153. [PubMed: 16748966]
11. Jencks WP. Chem Rev. 1972; 72:705–718.
12. Jencks WP. J Am Chem Soc. 1972; 94:4731–4732.
13. Dewar MSJ. J Am Chem Soc. 1984; 106:209–219.
14. All of our studies have been carried out on ketosteroid isomerase from *Pseudomonas putida*, also called pKSI. Some of the earlier studies mentioned in the Introduction and Discussion were carried out on the homolog from *Comamonas testosteroni*, called tKSI. In general, the kinetics and mechanism of wild-type pKSI and tKSI are known to be very similar.
15. Pollack R. Bioorg Chem. 2004; 32:341–353. [PubMed: 15381400]
16. Guthrie JP, Kluger R. J Am Chem Soc. 1993; 115:11569–11572.
17. Hawkinson DC, Eames TCM, Pollack RM. Biochemistry. 1994; 33:12172–12183. [PubMed: 7918439]
18. Kuliopolis A, Mildvan AS, Shortle D, Talalay P. Biochemistry. 1989; 28:149–159. [PubMed: 2706241]
19. Kim SW, Cha S-S, Cho H-S, Kim J-S, Ha N-C, Cho M-J, Joo S, Kim KK, Choi KY, Oh B-H. Biochemistry. 1997; 36:14030–14036. [PubMed: 9369474]
20. Pollack RM, Zeng B, Mack JPG, Eldin S. J Am Chem Soc. 1989; 111:6419–6423.
21. Yun YS, Lee T-H, Nam GH, Jang DS, Shin S, Oh B-H, Choi KY. J Biol Chem. 2003; 278:28229–28236. [PubMed: 12734184]
22. Kuliopolis A, Talalay P, Mildvan AS. Biophys J. 1990; 57:39a.
23. Xue L, Talalay P, Mildvan AS. Biochemistry. 1990; 29:7491–7500. [PubMed: 2223781]
24. Gerlt JA, Kozarich JW, Kenyon GL, Gassman PG. J Am Chem Soc. 1991; 113:9667–9669.
25. Gerlt JA, Gassman PG. J Am Chem Soc. 1992; 114:5928–5934.
26. Hand ES, Jencks WP. J Am Chem Soc. 1975; 97:6221–6230.
27. Hegarty AF, Jencks WP. J Am Chem Soc. 1975; 97:7188–7189.
28. Zeng B, Bounds PL, Steiner RF, Pollack RM. Biochemistry. 1992; 31:1521–1528. [PubMed: 1346570]
29. Petrounia IP, Pollack RM. Biochemistry. 1998; 37:700–705. [PubMed: 9425094]
30. Childs W, Boxer SG. Biochemistry. 2010; 49:2725–2731. [PubMed: 20143849]

31. Kraut DA, Sigala PA, Pybus S, Liu CW, Ringe D, Petsko GA, Herschlag D. *PLoS Biol.* 2006; 4:501–519.
32. Zeng B, Pollack RM. *J Am Chem Soc.* 1991; 113:3838–3842.
33. Schwans JP, Kraut DA, Herschlag D. *Proc Natl Acad Sci USA.* 2009; 106:14271–14275. [PubMed: 19706511]
34. Weinkam P, Zimmermann J, Sagle LB, Matsuda S, Dawson PE, Wolynes PG, Romesberg FE. *Biochemistry.* 2008; 47:13470–13480. [PubMed: 19035653]
35. Miller CS, Corcelli SA. *J Phys Chem B.* 2009; 113:8218–8221. [PubMed: 19463012]
36. Suydam I, Boxer SG. *Biochemistry.* 2003; 42:12050–12055. [PubMed: 14556636]
37. Zierkiewicz W, Michalska D, Czarnik-Matusiewicz B, Rospenk M. *J Phys Chem A.* 2003; 107:4547–4554.
38. McIntosh LP, Hand G, Johnson PE, Joshi MD, Korner M, Plesniak LA, Ziser L, Wakarchuk WW, Withers SG. *Biochemistry.* 1996; 35:9958–9966. [PubMed: 8756457]
39. Chivers PT, Prehoda KE, Volkman BF, Kim B-M, Markley JL, Raines RT. *Biochemistry.* 1997; 36:14985–14991. [PubMed: 9398223]
40. [http://enzyme.ucd.ie/cgi-bin/titration\\_db/main.cgi](http://enzyme.ucd.ie/cgi-bin/titration_db/main.cgi)
41. Kukic P, Farrell D, Søndergaard CR, Bjarnadottir U, Bradley J, Pollastri G, Nielsen JE. *Proteins.* 2009; 78:971–984. [PubMed: 19894279]
42. Malhorta SK, Ringold HJ. *J Am Chem Soc.* 1965; 87:3228–3236.
43. Xue L, Kuliopulos A, Mildvan AS, Talalay P. *Biochemistry.* 1991; 30:4991–4997. [PubMed: 2036366]
44. Fafarman AT, Sigala PA, Fenn TD, Herschlag D, Boxer SG. *Proc Natl Acad Sci USA.* In Press.
45. Röthlisberger D, Khersonsky O, Wollacott AM, Jiang L, DeChancie J, Betker J, Gallaher JL, Althoff EA, Zanghellini A, Dym O, Albeck S, Houk KN, Tawfik DS, Baker D. *Nature.* 2008; 453:190–195. [PubMed: 18354394]
46. Seebeck F, Hilvert D. *J Am Chem Soc.* 2005; 127:1307–1312. [PubMed: 15669871]

**Figure 1.**

(A) Mechanism of KSI: 5-androsten-3,17-dione, the steroid substrate is converted to the conjugated isomer, 4-androsten-3,17-dione, via the enolization (first step) and re-ketonization (second step) of the carbonyl. The identity of the intermediate could be a dienolate (top), or a dienol (bottom) if concerted proton transfer occurred. (B) A thermodynamic cycle between the KSI Michaelis complex, E•S, and two potential intermediates: path (i) is a base-mediated proton abstraction forming a dienolate, and path (ii) is a concerted acid-base reaction forming a dienol. (C) Internal proton transfer between the KSI oxyanion hole and a bound ligand.

**Figure 2.**

(A) Normalized IR spectra of 4-fluorophenol dissolved in water, pH 2 (red), and dissolved in  $\text{CCl}_4$  (black). Additionally, in  $\text{CCl}_4$  one is able to observe an O-H bending mode (at  $1173.9\text{ cm}^{-1}$ , as assigned by calculations<sup>37</sup>) which vanishes upon transfer to aqueous medium. (B) IR spectra of 4-fluorophenol (3.0 mM, pH 2, .01 M HCl) in red, and 4-fluorophenoxide (3.0 mM, pH 14, 1 M KOH) in blue. The overtone at  $1200\text{ cm}^{-1}$  has a strong Fermi resonance with the C-F stretch at  $1221\text{ cm}^{-1}$ , and “borrows” intensity from the C-F stretch. (C) IR spectrum of 4-fluorophenol bound to  $\text{KSI}^{\text{D40N}}$ , in 40 mM  $\text{KP}_i$ , pH 7.2 ([ligand] = 3.0 mM, [KSI] = 4.7 mM). (D) Normalized IR spectra of 4-fluorophenol-2,6- $d_2$  dissolved in water, pH 2 (red), and dissolved in  $\text{CCl}_4$  (black). Based on previous calculations,<sup>37</sup> we tentatively assign the peak at  $1142\text{ cm}^{-1}$  to the O-H bending mode, which vanishes upon transfer to aqueous medium. (E) IR spectra of 4-fluorophenol-2,6- $d_2$  (3.0 mM, pH 2, .01 M HCl) in red, and 4-fluorophenoxide-2,6- $d_2$  (3.0 mM, pH 14, 1 M KOH) in blue. The C-F band red-shifts from  $1190.0\text{ cm}^{-1}$  to  $1175.7\text{ cm}^{-1}$  in the anion, and grows 1.8 times in integrated intensity. (F) IR spectrum of 4-fluorophenol-2,6- $d_2$  bound to  $\text{KSI}^{\text{D40N}}$  (black), in 40 mM  $\text{KP}_i$ , pH 7.2 ([ligand] = 3.0 mM, [KSI] = 7.4 mM).

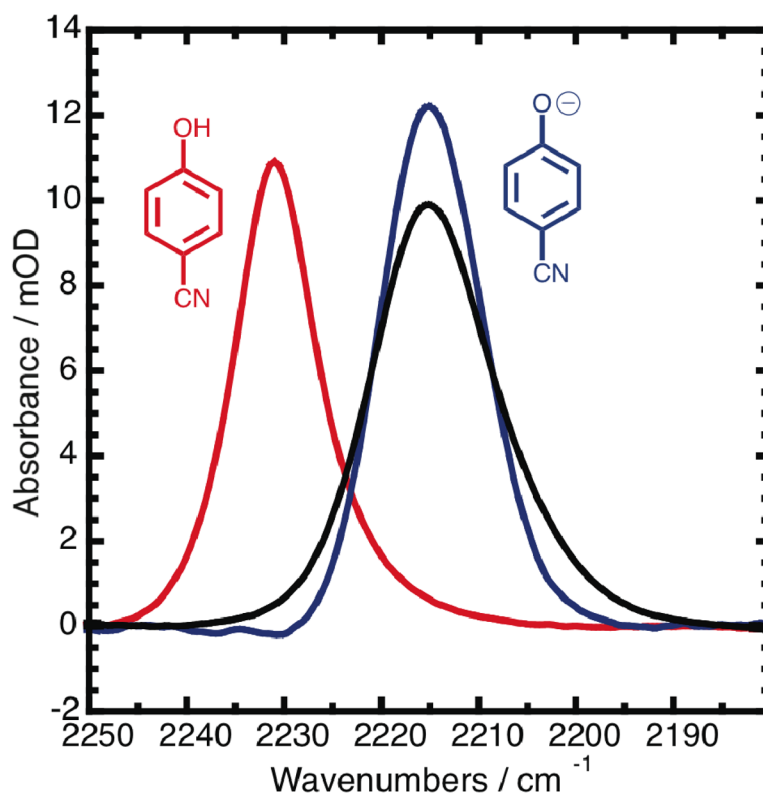


**Figure 3.** IR spectra of 4-cyanophenol (3.0 mM, pH 2, .01 M HCl) in red, and 4-cyanophenoxide (3.0 mM, pH 14, 1 M KOH) in blue. IR spectrum of 4-cyanophenol bound to KSI<sup>D40N</sup> (black), in 40 mM CHES, pH 9.0 ([ligand] = 3.0 mM, [KSI] = 4.7 mM).

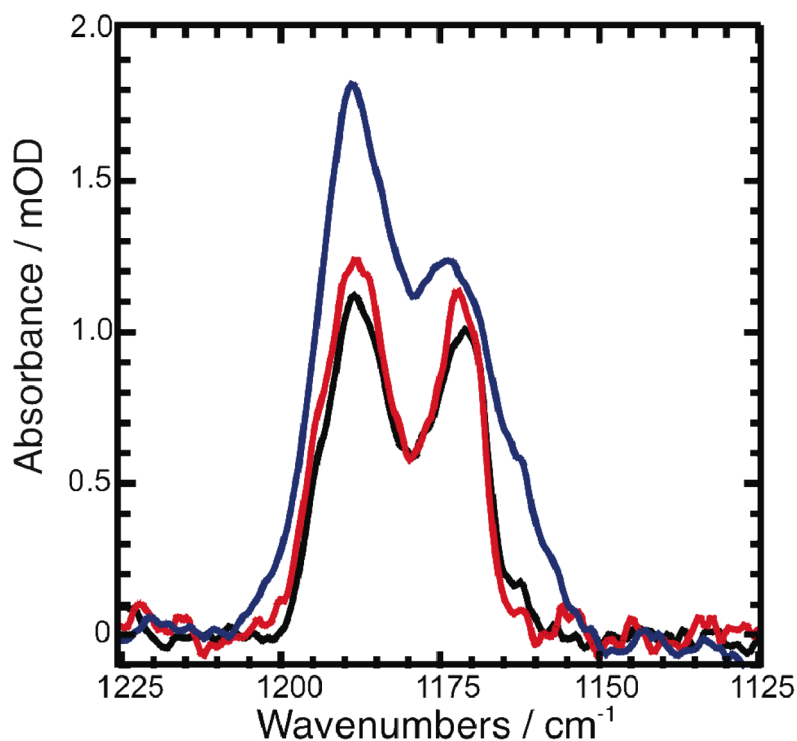


**Figure 4.** Concentration dependence of the IR spectra of 4-fluorophenol-2,6- $d_2$  bound to KSI<sup>D40N</sup>. Black trace: [KSI] = 7.4 mM, [4Fd2] = 3.0 mM,  $f_{\text{bound}} = .97$ ,  $f_{\text{obs}} = .29$ ,  $f = .30$ . Red trace: [KSI] = 4.7 mM, [4Fd2] = 3.0 mM,  $f_{\text{bound}} = .92$ ,  $f_{\text{obs}} = .26$ ,  $f = .28$ . Blue trace: [KSI] = 4.7 mM, [4Fd2] = 5.0 mM,  $f_{\text{bound}} = .80$ ,  $f_{\text{obs}} = .24$ ,  $f = .29$ .  $f_{\text{bound}}$  is the fraction of ligand that is bound, and is calculated from the  $K_D$  at pH 7.2 ( $150 \mu\text{M}^3$ ).  $f_{\text{obs}}$  is the fraction of ligand ionized.  $f$  is the fraction of *bound* ligand that is ionized, determined by subtracting the contribution from unbound ligand.



**Table 1**

Summary of FTIR data of 4-fluorophenol and 4-cyanophenol

System <sup>a</sup>	Peak Position / cm <sup>-1</sup>	FWHM / cm <sup>-1</sup>	Max / mOD
4-fluorophenol $\bar{\nu}$ (C-F)			
CCl <sub>4</sub>	1226.5	8.67	
pH 2	1221.2 ± .3	9.61	1.1
pH 2 <sup>b</sup>	1200.6 ± .1	9.33	1.6
pH 14	1199.1 ± .1	13.89	4.9
KSI-bound, peak 1	1221.9 ± .4	16.13	1.3
KSI-bound, peak 2	1201.0 ± 2	12.04	1.4
4-cyanophenol $\bar{\nu}$ (C-N)			
pH 2	2230.9 ± .07	10.01	10.9
pH 14	2215.1 ± .05	12.38	12.2
KSI-bound	2215.1 ± .06	14.84	10.0

<sup>a</sup>Details of the system conditions are described in caption of Figures 2 and 3.

<sup>b</sup>Fermi resonance peak.

**Table 2**Summary of FTIR data of 4-fluorophenol- $D_2$ 

System <sup>a</sup>	Peak Position / $\text{cm}^{-1b}$	FWHM / $\text{cm}^{-1c}$	Intensity <sup>d</sup>
<b>4-fluorophenol-<math>d_2</math> <math>\bar{\nu}</math> (C-F)</b>			
$\text{CCl}_4$	1192.4	4.73	
pH 2	$1190.0 \pm .1$	10.40	1.6 (.0199)
pH 14	$1175.7 \pm .3$	15.38	2.0 (.0370)
KSI-bound, peak 1	$1188.5 \pm .3$	8.81	1.1
KSI-bound, peak 2	$1171.1 \pm .5$	7.18	1.0
KSI-bound, fit 1 <sup>e</sup>	1187.9	12.42	1.11 (.0146)
KSI-bound, fit 2 <sup>e</sup>	1171.9	10.58	1.00 (.0113)

<sup>a</sup>Details of the system conditions are described in caption of Figure 3.

<sup>b</sup>Peak positions are reported of the spectral average from three repeats. Error bars are the standard deviation of the peak position from the three repeats.

<sup>c</sup>Full width at half maxima (FWHM) are reported of the spectral average from three repeats.

<sup>d</sup>The intensity of the maximum in mOD, followed by the integrated intensity over the whole band in  $\text{mOD} \times \text{cm}^{-1}$  in parentheses. For the basis spectra, integrated intensities are calculated using the trapezoidal technique over the lineshape; for the Gaussian fits, they are calculated analytically.

<sup>e</sup>These parameters reflect the set of two Gaussians that best fit the observed spectrum according to the Levenberg-Maquardt algorithm.